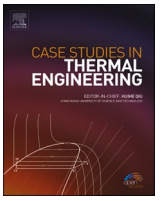
Case Studies in Thermal Engineering 74 (2025) 106887



Contents lists available at ScienceDirect

Case Studies in Thermal Engineering

journal homepage: www.elsevier.com/locate/csite



Measurement of thermal conductivity using 2D inverse heat conduction problem approach by identifying simultaneously the heat dissipation phenomena

Ari Satmoko [a,b], Engkos Achmad Kosasih [a,*], Anhar Riza Antariksawan [c], Muhsin Kılıç [d], Ahmad Zikri [e], Muhammad Ainun Al Ghafari [a], Muflikh Kas Yudamaulana [a], Seli Siti Sholihat [f]

[a] Department of Mechanical Engineering, Universitas Indonesia, Depok, 16424, West Java, Indonesia
[b] Research Centre for Nuclear Beam Analysis Technology, National Agency for Research and Innovation, Serpong, Indonesia
[c] Polytechnique Institute of Nuclear Technology, National Agency for Research and Innovation, Yogyakarta, Indonesia
[d] Department of Mechanical Engineering, Faculty of Engineering, Bursa Uludag University, Bursa, 16059, Türkiye
[e] Department of Mechanical Engineering, Faculty of Engineering, Universitas Sumatera Utara, Medan, 20155, Indonesia
[f] Gunadarma University, Depok, Indonesia

ARTICLE INFO

Keywords:
Conjugate gradient method
Inverse heat conduction problems (IHCP)
Thermal conductivity
2D heat transfer
Thin plate

ABSTRACT

Various methods for measuring thermal conductivity have been applied under both steady-state and transient conditions. A challenge in thermal conductivity measurement lies in accurately identifying the heat dissipated to the environment. This inaccuracy affects the calculation of a material's thermal conductivity. To address this challenge, a method based on a two-dimensional inverse heat conduction problem (2D IHCP) was developed to simultaneously evaluate the thermal conductivity of the material and determine the heat dissipation coefficient. So that, prior characterization of heat dissipation is no longer required. Compared to conventional measurement techniques, the advantage of this new method is improved measurement precision, as it can eliminate potential inaccuracies in identifying heat loss to the surroundings. This method proposes an algorithm for simultaneously determining thermal conductivity and the dissipation coefficient. The experimental validation using titanium plate material produced relatively satisfactory results, with deviations below 11.3 %. There is a tendency that the higher the applied heater power, the closer the predicted thermal conductivity of titanium approaches the vendor's reference value. The current research is limited to steady-state problems in two-dimensional thin plates.

Nomenclature

A	Area [m^2]
A_{diss}	Area in which heat is dissipated [m^2]
d^k	Direction of descent at k-iteration
e	Thickness of the plate [m]
h_{diss}	Dissipation coefficient [$W/m^2.°C$]

(*continued on next page*)

* Corresponding author.
E-mail address: kosri@eng.ui.ac.id (E.A. Kosasih).

https://doi.org/10.1016/j.csite.2025.106887
Received 10 May 2025; Received in revised form 30 July 2025; Accepted 13 August 2025
Available online 30 August 2025
2214-157X/© 2025 The Authors. Published by Elsevier Ltd. This is an open access article under the CC BY license (http://creativecommons.org/licenses/by/4.0/).

(*continued*)

$\boldsymbol{J}$	Sensitivity matrix
k	Iteration number
k_p	Thermal conductivity of material [W/m.°C]
k_x	Mesh division in X-direction
k_y	Mesh division in Y-direction
L_x	Length of the plate [m]
L_y	Width of the plate [m]
$\mathrm{n_m}$	Number of measurement points
n	Number of discretization nodes
(n,n)	Matrix dimension (n,n)
P	Matrix with dimension (n,n)
q	Heat flux [W/m^2]
$\dot{Q}_{diss}$	Heat dissipated from the plate to environ [W/m^2]
$\dot{Q}_{ext}$	Heat produced by electrical heater [W/m^2]
$S_{ML}(k_p,h_{diss})$	Sum of least square between calculation and measurement temperatures
$[]^T$	Matrix transpose
$T(x,y)$	Temperature at (x,y) coordinate [°C]
$\boldsymbol{T}(k_p,h_{diss})$	Temperature distribution in function of k_p and h_{diss} [°C]
T_a	Ambient temperature [°C]
x	X-direction
$\boldsymbol{X}$	Temperature vector
y	Y-direction
$\boldsymbol{Y}$	Measurement temperature vector
$\boldsymbol{Y_H}$	External heat vector
β^k	Search step size at k-iteration
γ^k	Conjugation coefficient at k-iteration
ε	Finite difference step coefficient
σ	Standard deviation for measurement error
$\boldsymbol{\xi}$	Measurement tolerance
$\nabla\ S_{ML}(k_p,h_{diss})$	Gradient direction

1. Introduction

Various new materials have been developed to meet growing demands. For industrial applications involving heat processes, one of the technical specifications of construction materials is thermal conductivity (k_p). Materials with high thermal conductivity easily transfer heat and are ideal as heat conductors. Conversely, materials with low thermal conductivity are suitable for use as thermal insulators. Thermal conductivity can be measured using various methods. These methods are classified into two categories: steady state and transient [1].

The steady state approach utilizes Fourier's law by calculating the temperature gradient of heat flow under constant conditions. Within this category are the radial heat flow method (ISO 8497:1994), comparative cut bar method (ASTM E1225-13), guarded heat flow meter method (ASTM E1530-19), and guarded hot plate method (ASTM C177-19 and ISO 8302). Both comparative and absolute models are available. The comparative model uses a reference sample with a known thermal conductivity, while the absolute model involves measuring the heat flux from the power of the heater used. The guarded hot plate (GHP) or heat flow meter (HFM) methods are the most commonly used to measure thermal conductivity and thermal resistance for insulators [2]. Among steady state techniques, the GHP method is considered the most accurate. However, it requires large specimen sizes. Many researchers have employed these standard methods to measure the thermal conductivity of materials. In Ref. [3] to test the thermal properties of bio-based straw materials, the HFM was modified using a temperature-controlled chamber. The modification aimed to ensure a stable and controlled temperature difference during testing, as the specimen is enclosed in a sealed chamber.

Transient methods have increasingly gained researchers' attention. In transient techniques, temperature changes over time are measured while heat is applied either periodically or in pulses. Transient methods include the hot wire method (ASTM C1113/C1113M − 09 and ISO 8894–1:2010), thermal probe method (ASTM D5334-14), transient plane source (TPS) method (ISO 22007–2:2015) [4,5], and laser flash method (ASTM E1461-13 and ISO 22007–4:2017). The thermal probe is robust and difficult to damage. However, if the probe diameter is too large, significant axial heat loss can reduce measurement accuracy. The TPS method has limitations due to its requirement for a double sample. The modified transient plane source (MTPS) was developed for more flexibility, requiring only a single sample (ASTM D7984-16). The laser flash method uses laser light to heat the specimen (ASTM E1461-13 and ISO 22007–4:2017). Advantages of the laser flash method include the need for only a small sample size, short measurement time, and the ability to operate over a wide temperature range. The non-contact nature of laser heating and temperature sensing also avoids the effects of contact thermal resistance found in other methods. However, thermal conductivity measurement is indirect, as specific heat capacity and sample density must be determined through separate experiments, which may introduce significant error. The laser flash method also requires a certain sample thickness, limiting its use for thin films.

Both steady state and transient methods have their advantages and limitations, and each is only suitable for a limited range of materials depending on thermal properties, sample configuration, and measurement temperature [6]. Among the various thermal conductivity measurement methods, there is no universal technique. The selection of a measurement technique must consider sample properties, test procedures, and potential sources of error that could affect the final results, such as heat loss from convection and

radiation [7]. For high-temperature thermal conductivity measurements, adequate international standards are practically unavailable, and most of these instruments have been self-developed by universities and materials testing laboratories material [8]. M. Janek et al. [9] conducted several design modifications in measuring the thermal conductivity of polyurethane composites.

Recently, the inverse heat conduction problem (IHCP) has become a growing area of research, particularly for its application in characterizing the thermal properties of materials. IHCP refers to a heat conduction problem where the effect of temperature is known, but the cause is unknown. Various problems have been addressed using IHCP principles, such as estimation of heat sources [10], characterization of thermal properties of materials (R.N. Prithiviraajan et al. [11]), estimation of heat transfer coefficients at contact surfaces, estimation of convection coefficients, non-destructive testing (J. Zhang et al. [12]), and others. Thomas et al. [13] developed an experimental setup to estimate the thermal properties of composite materials by solving the IHCP. The direct problem was solved using a 3-D finite element solver. Chanda et al. [14] conducted a similar study for anisotropic composites using a three-dimensional finite difference method. IHCP was solved using artificial neural networks (ANN) trained with the Levenberg–Marquardt algorithm (LMA). Maneesh V. et al. [15] proposed a combined methodology using ANSYS software and ANN. A. Saad et al. [16] employed the inverse Gauss–Newton–Levenberg–Marquardt method to identify the thermal conductivity of fibre-reinforced bars. J. Zhang et al. [17] investigated the temperature-dependent thermal conductivity of copper oxide materials using both gradient-based and stochastic algorithms. Yurii M. Matsevytyi et al. [18] identified thermophysical characteristics using A.N. Tikhonov's regularization approach. The IHCP is applied to identify the temperature-dependent thermal conductivity tensor, with known heat capacity and boundary conditions. L. Yang et al. [19] estimated transient thermal conductivity using an improved artificial bee colony algorithm. S. Somasundharam et al. [20] conducted laboratory experiments using an IR camera to monitor temperature. The 3-D transient IHCP model was solved using a combination of finite volume methods and the Levenberg–Marquardt algorithm. Sun S. et al. [21] used the Particle Swarm Optimization Algorithm to evaluate the temperature-dependent thermal properties of biological tissue. Shuangcheng Sun [22] employed a hybrid optimization technique, which combines the decentralized fuzzy inference method (DFIM) and the sequential quadratic programming (SQP) algorithm, to simultaneously reconstruct the thermal boundary conditions and the physical properties of the participating medium.

Despite the availability of standardized techniques, a major challenge in determining thermal conductivity lies in the dissipation of heat to the environment. Researchers have attempted to address this by modifying the design of test structures and using more accurate data acquisition systems. Heat leakage is inevitable and interferes with the calculation of a material's thermal conductivity. Characterization of the testing conditions is typically performed in advance to determine operational parameters. However, replicating the same operational conditions during the actual thermal conductivity measurement can be difficult. Although IHCP techniques have been widely applied, they have not yet resolved the issue of heat dissipation, which can significantly affect the precision of thermal conductivity measurements.

Conventional methods for measuring the thermal conductivity of materials still face challenges due to heat losses that are either neglected or unaccounted for, reducing the accuracy of the final thermal conductivity calculations. To address this issue, a 2D IHCP-based thermal conductivity measurement method has been developed enabling the simultaneous evaluation of a material's thermal conductivity and heat dissipation coefficient. Various techniques exist to solve inverse problems, each with its own advantages and limitations. In this study, the conventional Conjugate Gradient Method was employed. By simultaneously estimating both thermal conductivity and dissipation coefficient, the method eliminates the need for prior heat dissipation characterization, thereby improving calculation accuracy. The method involves a thin plate equipped with several thermocouples to monitor temperature distribution. Based on the measured temperatures, the inverse method is used to determine thermal conductivity. Compared to conventional approaches, the proposed method offers a significant advantage by accounting for heat losses that are typically overlooked. This paper presents the development of the algorithm for jointly solving thermal conductivity and heat dissipation coefficient, along with its validation using experimental data. The current scope of the research is limited to steady-state problems in two-dimensional thin plates.

2. Methodology

A study was conducted to apply IHCP in predicting the thermal conductivity of a plate under 2D steady-state condition. There are two main activities: experiments and numerical computations. The numerical computations include forward heat conduction and

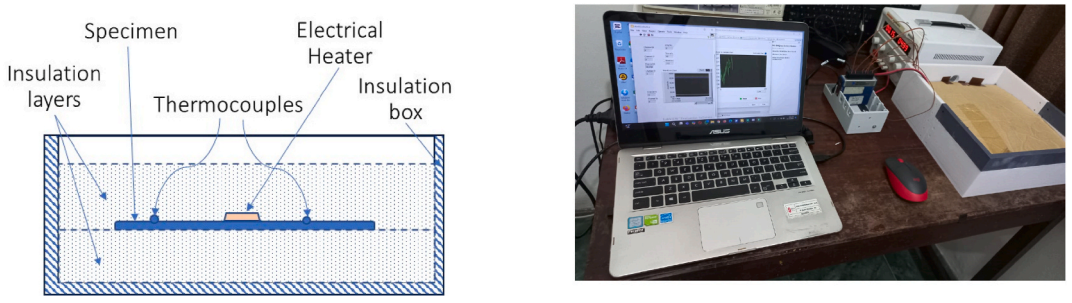


Fig. 1. Experimental configuration (left) and set up (right).

IHCP solution algorithms.

2.1. Experimental setup

Fig. 1 illustrates the experimental configuration and setup. The specimen is a titanium plate. The plate is positioned horizontally with dimensions of 16.0 × 20.0 cm^2 and a thickness of 1 mm. To insulate the surface, white glass wool is used. Four thermocouple sensors are placed on the plate. A heat flux is generated by an electric heater measuring 3.5 × 2.1 cm^2. The temperature changes of the plate are recorded by NI module calibrated with a mercury thermometer ranging from 0 to 150 °C with the accuracy of 0.2 °C.

2.2. Forward heat conduction

The similar configuration as shown in Fig. 1 is also discussed in the application of IHCP for heat flux estimation [23]. The heat balance equation under steady condition on a rectangular plate with length L_x, width L_y and thickness e is shown in Equation 1

$$\frac{\partial^2 T(x,y)}{\partial x^2}+\frac{\partial^2 T(x,y)}{\partial y^2}=0, \text{for } 0 < x < L_x \ \& \ 0 < y < L_y \tag{1}$$

where $T(x,y)$ is the temperature at coordinates (x,y). An electric heater supplies external heat flux, $\dot{Q}_{ext}$ causing the increase of the plate temperature from the initial to the plate temperature, $T(x,y)$. Amount of heat will be dissipated to the surrounding, $\dot{Q}_{diss}$. At steady state, thermal equilibrium will occur. For given areas, boundaries conditions are applied. The heater only provides heat flux in the area where the heater is attached to the plate, so that:

$$\dot{Q}_{ext}=q, \text{at heater area} \tag{2}$$

where q is the heat flux from the heater. In the steady state, heat flows from the plate to the insulation through conduction, and then from the insulation surface to the environment through convection and radiation. In this study, the combination of heat loss from the plate through these two modes of heat transfer is modelled as heat dissipation and is mathematically represented by Equations (3)–(5).

$$\dot{Q}_{diss}=A_{diss}\ h_{diss}(T(x,y)-T_a), \text{for } A_{diss} \tag{3}$$

where A_{diss} is the dissipation area, h_{diss} is dissipation coefficient and T_a is ambient temperature. The dissipation phenomenon is also assumed to occur on all four sides of the plate:

$$k_p\frac{\partial T(x,y)}{\partial x}=e\,L_y\,h_{diss}(T(x,y)-T_a), \text{for } x=0 \text{ and } x=L_x \tag{4}$$

$$k_p\frac{\partial T(x,y)}{\partial y}=e\,L_x\,h_{diss}(T(x,y)-T_a), \text{for } y=0 \text{ and } y=L_y \tag{5}$$

where k_p is the thermal conductivity.

The Finite Difference Method (FDM) solves the above heat conduction problems. Smaller rectangular elements discretize Equations (1)–(5). The plate in 2D is meshed using k_x and k_y divisions respectively in x and y directions (Fig. 2). The mesh creates n nodes where n is $(k_x+1)*(k_y+1)$. Heat balance equations are created for each node [24]. This is leading to the linear matrix equation:

$$\boldsymbol{P.X}=\boldsymbol{Y_H} \tag{6}$$

where the matrix $\boldsymbol{P}$ is a matrix of size (n, n), $\boldsymbol{X}$ is the n-dimensional temperature vector, and $\boldsymbol{Y_H}$ is the external heat vector.

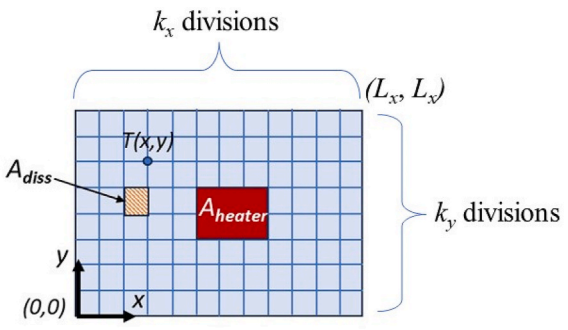


Fig. 2. Element discretization.

2.3. Inverse heat conduction problem

Some techniques for resolving the IHCP are discussed by M. N. Ozisik et al. [25] by introducing an objective function, S_{ML}:

$$S_{ML}(k_p,h_{diss}) = [\mathbf{Y} - \mathbf{T}(k_p,h_{diss})]^{\mathbf{T}} [\mathbf{Y}-\mathbf{T}(k_p,h_{diss})] \quad (7)$$

where $\boldsymbol{Y}$ is the measurement temperature data vector and $\boldsymbol{T}(k_p,h_{diss})$ is the solution of the mathematical formulation of the heat transfer problem obtained from the parameter k_p and h_{diss}. This objective function has two variables: k_p and h_{diss}. The solution is obtained by separating each variable, assuming the other variable is constant. In the first step, the objective function is minimized with respect to h_{diss}, assuming k_p is constant. In the second step, the objective function is minimized with respect to k_p, assuming h_{diss} is constant.

An iterative procedure to minimize the objective function is using the Conjugate Gradient Method (CGM). For the first step, we obtain Equation (8):

$$h_{diss}{}^{k+1} = h_{diss}{}^{k} - \beta^k d^k \text{ at } k_p \text{ constant} \quad (8)$$

with

$$d^k = \nabla S_{ML}(h_{diss}{}^{k}) + \gamma^k d^{k-1} \quad (9)$$

where k is the iteration number, β^k is the search step size, and γ is the conjugation coefficient. Term d^k is called as the direction of descent as the conjugation of the gradient direction $\nabla S_{ML}(h_{diss}{}^{k})$ and the direction of descent of the previous iteration, d^{k-1}. By developing the Taylor series and introducing the sensitivity matrix $\boldsymbol{J}$, the conjugation of the gradient direction is given by:

$$\nabla S_{ML}(h_{diss}{}^{k})^1 = -2(\boldsymbol{J}^k)^{\mathrm{T}} [\boldsymbol{Y} - \boldsymbol{T}(h_{diss}{}^{k})] \quad (10)$$

$$\boldsymbol{J} = [\partial \boldsymbol{T}(h_{diss}) / \partial h_{diss}]^{\mathrm{T}} \quad (11)$$

To evaluate the sensitivity coefficients $\boldsymbol{J}$, the central difference finite technique is used:

$$\boldsymbol{J} = [\boldsymbol{T}(h_{diss}{}^{\mathrm{k}} + \varepsilon\, h_{diss}{}^{\mathrm{k}}) - \boldsymbol{T}(h_{diss}{}^{\mathrm{k}})] / \varepsilon\, h_{diss}{}^{\mathrm{k}} \quad (12)$$

where, $h_{diss}{}^{\mathrm{k}}$ is the predicted dissipation coefficient in the $\mathrm{k}^{\text{-th}}$ iteration and $\varepsilon\, h_{diss}{}^{\mathrm{k}}$ is the finite difference step. The numerical computation continues iteratively and stops when the S_{ML} reaches a minimum or Equation (13) is satisfied:

$$S_{ML}(h_{diss}{}^{k+1}) > S_{ML}(h_{diss}{}^{k}) \quad (13)$$

In a similar way to Equation (8), for the second step we obtain Equation (14):

$$k_p{}^{k+1} = k_p{}^{k} - \beta^k d^k \text{ at } h_{diss} \text{ constant} \quad (14)$$

with other variables also identical.

Table 1
Typical S_{ML} variable values as a function of guessed k_p and h_{diss}.

h_{diss}	k_p									
	95	96	97	98	99	100	101	102	103	104
3.493	0.070	0.066	0.067	0.072	0.082	0.096	0.114	0.136	0.161	0.190
3.494	0.056	0.050	0.048	0.051	0.059	0.071	0.086	0.106	0.129	0.155
3.495	0.047	0.038	0.034	0.034	0.040	0.049	0.063	0.080	0.101	0.125
3.496	0.041	0.030	0.023	0.021	0.024	0.031	0.043	0.058	0.076	0.098
3.497	**0.039**	0.025	0.016	**0.012**	0.013	0.018	0.027	0.039	0.056	0.075
3.498	0.042	0.025	0.014	0.007	0.005	0.008	0.014	0.025	0.039	0.057
3.499	0.048	0.029	0.015	**0.006**	**0.002**	0.002	0.006	0.015	0.027	0.042
3.500	0.068	0.036	0.020	0.009	0.002	**4E-09**	0.002	0.008	0.018	0.031
3.501	0.072	0.048	0.029	0.015	0.006	0.002	0.002	0.006	0.013	0.024
3.502	0.090	0.063	0.042	0.026	0.015	0.008	0.005	0.007	0.012	0.021
3.503	0.112	0.083	0.059	0.040	0.027	0.018	0.013	0.012	0.015	0.022
3.504	0.138	0.106	0.080	0.059	0.043	0.031	0.024	0.021	0.022	0.027
3.505	0.157	0.133	0.104	0.081	0.063	0.049	0.040	0.034	0.033	0.036
3.506	0.201	0.164	0.133	0.107	0.086	0.070	0.059	0.051	0.048	0.048
3.507	0.238	0.199	0.165	0.137	0.114	0.096	0.082	0.072	0.067	0.065
3.508	0.279	0.238	0.202	0.171	0.145	0.125	0.109	0.097	0.089	0.085
3.509	**0.324**	0.280	0.242	0.209	0.181	0.158	0.139	0.125	0.116	0.110

The acceptability of the calculation results is determined using the following criteria:

$$S_{ML}(k_p{}^{k+1}, h_{diss}{}^{k+1}) < \xi \tag{15}$$

where ξ is the tolerance. By assuming σ is the standard deviation of the measurement error, $S_{ML}(k_p{}^{k+1}, h_{diss}^{k+1})$ should be lower than ξ, that is:

$$\xi = n_m \sigma^2 \tag{16}$$

where n_m is the number of the measurement points.

2.4. Parameter search algorithm using objective minimum function

In this numerical computation, the implementation of IHCP aims to determine simultaneously two parameters: k_p and h_{diss}. Table 1 shows typical S_{ML} values as a function of guessed k_p and h_{diss} for a material with actual $k_p = 100$ W/m°C and $h_{diss} = 3.5$ W/m$^{2\circ}$C. Fig. 3 visualizes the existence of a global minimum point for S_{ML}.

Searching for a minimum point involving two variables simultaneously carries the risk of being trapped in an undesired local minimum. To avoid this, the search is carried out in a step-by-step and iterative manner: first, h_{diss} is searched so that a local minimum S_{ML} point is obtained assuming constant k_p, followed by searching k_p so that a local minimum S_{ML} point is obtained assuming constant h_{diss}. These steps are repeated until the global minimum S_{ML} point is found.

As an illustration, suppose the initial guesses for k_p and h_{diss} are 95 W/m°C and 3.509 W/m$^{2\circ}$C, respectively (see Table 1). At this point, the value of the S_{ML} is 0.324. Assuming k_p is constant, the search iteration for the minimum S_{ML} leads to a h_{diss} value of 3.497, where the S_{ML} value becomes 0.039. Next, with h_{diss} held constant, the search for the minimum S_{ML} leads to a k_p value of 98 W/m°C, where the S_{ML} value changes to 0.012. The iterations continue until the global minimum S_{ML} is reached, with k_p equal to 100 W/m°C and h_{diss} equal to 3.5 W/m$^{2\circ}$C.

Our preliminary studies show that if the initial guesses for h_{diss} or k_p are too far off, the CGM iteration may fail to converge. Therefore, initial guesses for both k_p and k_p must not be arbitrary. For this reason, engineering justification is applied. Temperature measurements are taken at four points on the plate. The experiment also provides information on the heating power or heat flux. These temperature measurements and heat flux data can be used to predict the initial guesses. The h_{diss} is defined as the amount of heat lost divided by the temperature difference between the plate and the surrounding environment. An initial value for h_{diss} can then be determined. Meanwhile, the initial guess for k_p can be estimated using the measured temperature difference and distances between points.

From Table 1, there are two options to approach the global minimum point: either assuming k_p or h_{diss} as fixed first. Theoretically, both approaches will eventually lead to the same global minimum solution for S_{ML}. By choosing one of these options, the algorithm for determining k_p and h_{diss} to minimize S_{ML} is as follows.

i. Predict initial values of k_p and h_{diss} based on measurement data.

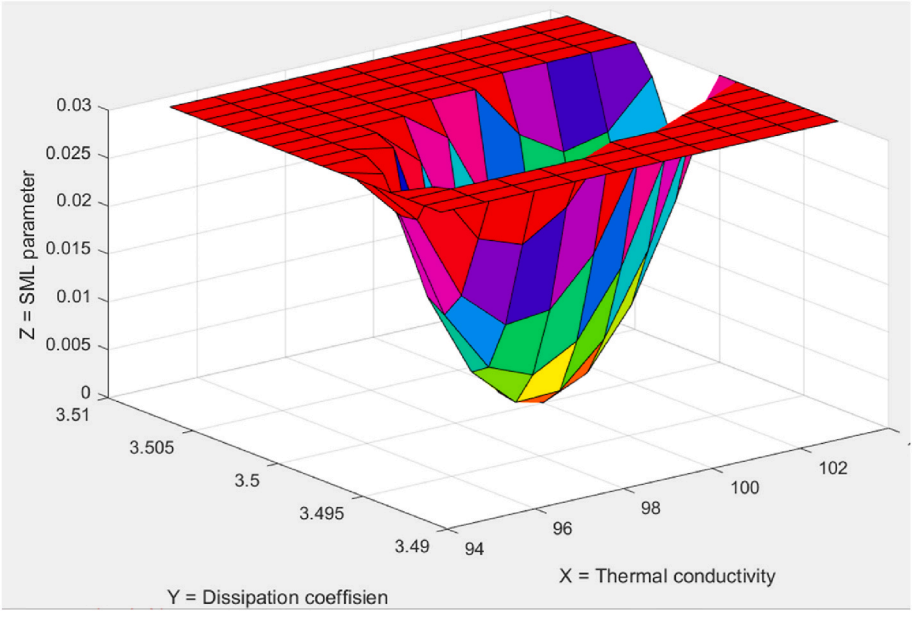


Fig. 3. Global minimum point of S_{ML}.

ii. Search for h_{diss} assuming k_p is given. If S_{ML} increases, stop the search.
iii. Search for k_p assuming h_{diss} is given. If S_{ML} increases, stop the search.
iv. Check the stopping criteria (i.e. $S_{ML}(k_p,h_{dis})^{i+1} > S_{ML}(k_p,h_{dis})^{i}$):
   - If not satisfied: return to step ii
   - If satisfied: stop
v. Check the acceptance criteria: if Equations (15) and (16) are satisfied, the result is considered acceptable.

Fig. 4 shows the flowchart of the numerical computation. After establishing the mathematical model, initial guesses for k_p and h_{diss} are made. In the first step, assuming k_p is fixed, h_{diss} is optimized to minimize S_{ML} using the Conjugate Gradient Method. In the second stage, again assuming h_{diss} is fixed, k_p is optimized to minimize S_{ML}, also using the Conjugate Gradient Method. If the global minimum S_{ML} is achieved, the computation ends. The final guessed values of k_p and h_{diss} from the last iteration are considered the final solution. However, if the global minimum S_{ML} is not yet achieved, the computational iteration returns to the first step and repeats the process.

Before using experimental data, the effectiveness of the above method was first tested using synthetic data. This synthetic data was obtained from the simulation of the forward heat transfer equation. By assuming that the thermal conductivity and other parameters are known, Equations (1)–(5) were solved to obtain the temperature distribution across the entire plate. The temperatures at several points were then extracted and used as synthetic data.

3. Results

A numerical method was developed using MatLAB software. The numerical method includes a forward heat conduction solution using the finite difference method, and the conjugate gradient method to solve the IHCP. In relation to the forward equation, mesh sensitivity has been evaluated, leading to the conclusion that elements sized 1×1 mm^2 are sufficient to discretize the specimen plate. The application of the IHCP to predict unknown thermal conductivity was carried out based on the flowchart in Fig. 3. Initially, IHCP was solved by implementing synthetic data created from forward equation simulations. Furthermore, the ability of the IHCP approach to find k_p was tested with experimental data.

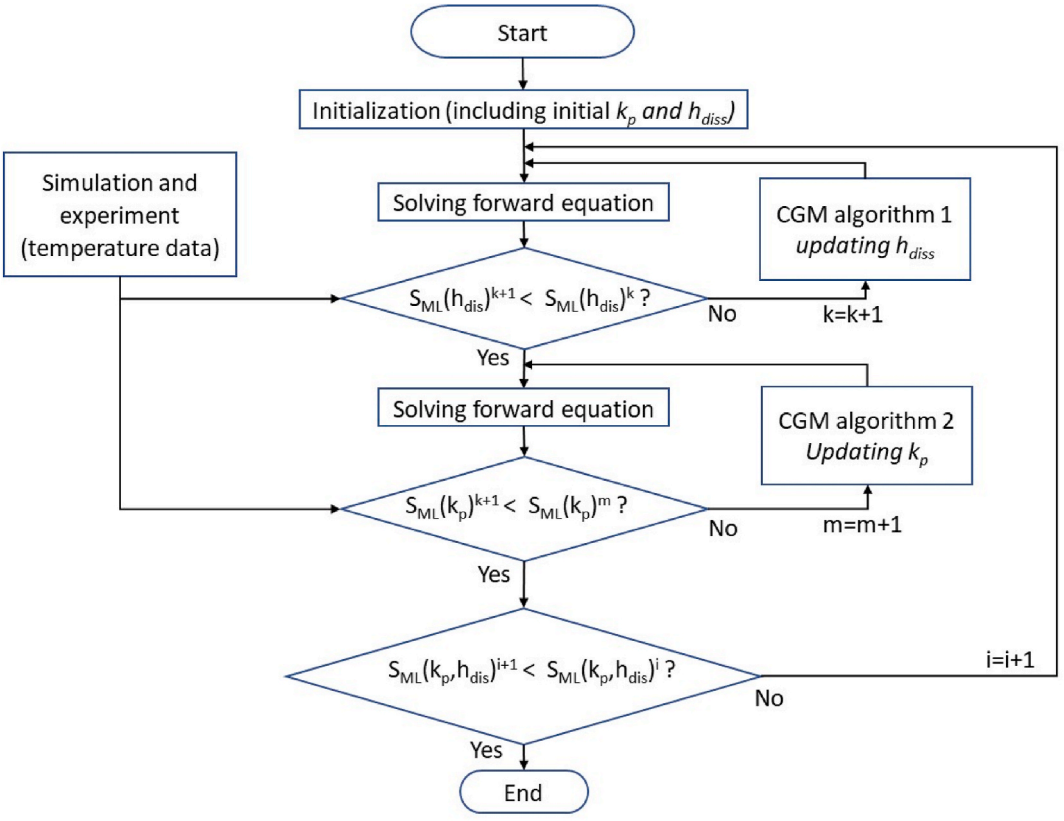


Fig. 4. Thermal conductivity prediction using the IHCP approach.

3.1. Prediction of thermal conductivity using synthetic data

3.1.1. Synthetic data from forward simulation

If the heat flux, heat dissipation coefficient, and all parameters involved in Equations (1)–(5) are known, the temperature distribution across the entire plate can be calculated. For example, a 3 × 2 cm^2 heater is attached to a plate with dimensions 16 × 16 cm^2. The heater produces heat at a rate of 12,500 W/m^2. Although insulated, heat still dissipates into the environment with a heat dissipation coefficient of 3.5 $W/m^{2\circ}C$. By solving the forward equations, the temperature distribution across the surface of the plate can be determined.

Fig. 5 shows the locations of the four temperature measurement points: P1(13.0; 6.0), P2(3.0; 5.0), P3(3.0; 12.0) and P4(15.0; 12.0). Three specimens made of different materials were studied. They had thermal conductivities of 10.0, 100.0, and 385, respectively. Table 2 presents the computed temperature data for materials with different thermal conductivities. The lower the thermal conductivity of the material, the more pronounced the temperature differences among the four points. The simulated temperature data are used as synthetic data for further analysis.

3.1.2. Thermal conductivity and dissipation coefficient as unknown parameter

By applying the algorithm from subsection 2.4, the IHCP CGM is used to determine the thermal conductivity k_p and the dissipation coefficient h_{diss}. Experimental measurements always contain errors. Therefore, the synthetic data in Table 2 is modified with randomly generated measurement errors. The IHCP method for predicting the thermal conductivity of specimen B is executed 100 times with specific levels of measurement error. Fig. 6 shows the impact of measurement errors on the deviation of the predicted k_p. A measurement error of ±0.1 °C results in a deviation of less than 10 %. For measurement errors of ±0.05 °C, ±0.02 °C, and ±0.01 °C, the deviations in k_p are below 5.5 %, 2.5 %, and 1.3 %, respectively.

Fig. 7 shows the deviation in predicted k_p values for specimens A, B, and C under a measurement accuracy of ±0.1 °C. It can be seen from the figure that materials with higher k_p values require higher precision in temperature measurements. For specimen A with a k_p value of 10 W/m·°C, the prediction accuracy is under 5 %. However, for specimen C with a k_p value of 385 W/m·°C, the deviation in the predicted k_p value is unsatisfactory, reaching up to 35 %.

In addition to k_p, numerical computation also evaluates h_{diss} and S_{ML}. In general, the deviation in the prediction of h_{diss} shows a similar pattern to that of k_p. For S_{ML} as a criterion of acceptability, all synthetic data result in calculations that meet the criteria defined in Equations (15) and (16).

3.2. Prediction of thermal conductivity using experiment data

3.2.1. Experiment

Four thermocouples were installed at the following coordinates: T1(10.0, 6.0), T2(12.0, 6.0), T3(14.0, 6.0), and T4(14.0, 2.0), as shown in Fig. 8. The experiment used a titanium plate with 99.5 % purity. Heater power was controlled via the input voltage setting. At each power level, the plate temperatures were recorded after reaching steady state. The results of the steady-state temperature measurements are shown in Fig. 9.

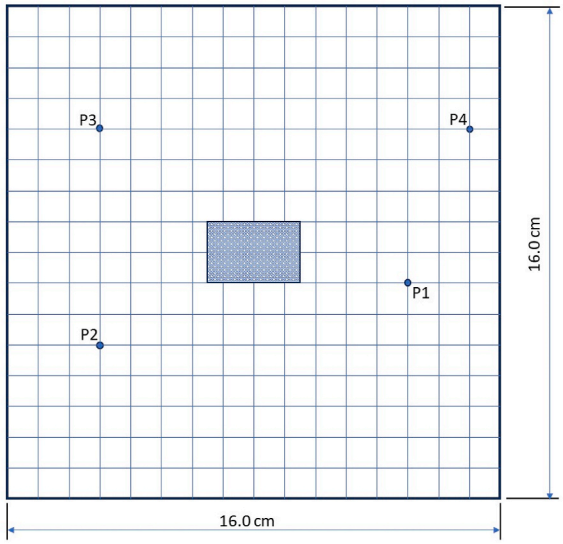


Fig. 5. Four temperature measurement locations on the plate: P1, P2, P3 and P4.

Table 2
Temperatures resulting from forward equation simulations as synthetic data.

No	Specimen	Dissipation coefficient (W/m^2.°C)	Thermal conductivity (W/m.°C)	Steady state temperature (°C)			
				P1	P2	P3	P4
1	A	3.5	10	103.527	98.473	93.178	85.195
2	B	3.5	100	108.236	107.568	106.854	105.768
3	C	3.5	385	108.555	108.377	108.187	107.897

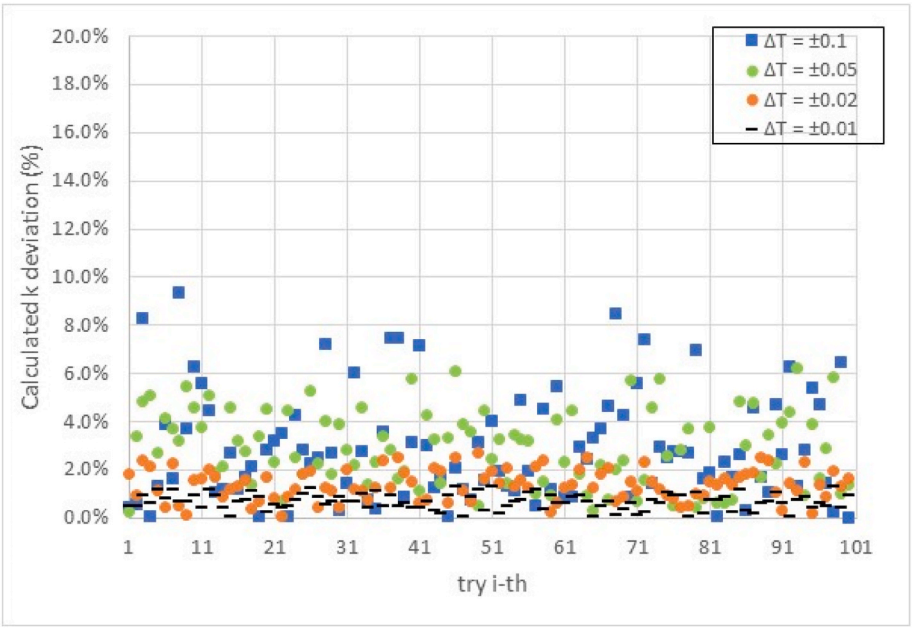


Fig. 6. Effect of temperature measurement error on the deviation of predicted k_p for specimen B.

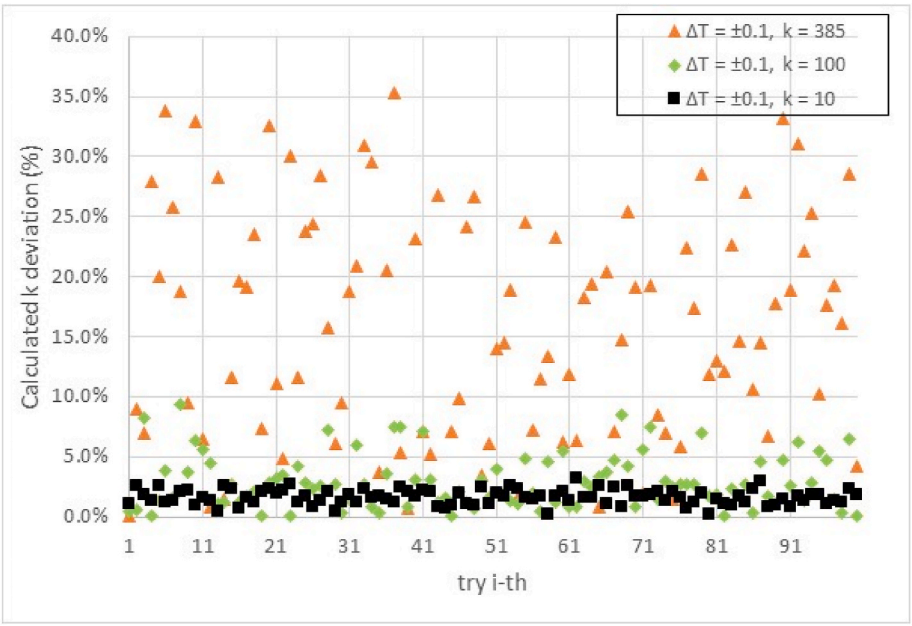


Fig. 7. Effect of thermal conductivity on the deviation in k_p prediction using the new algorithm.

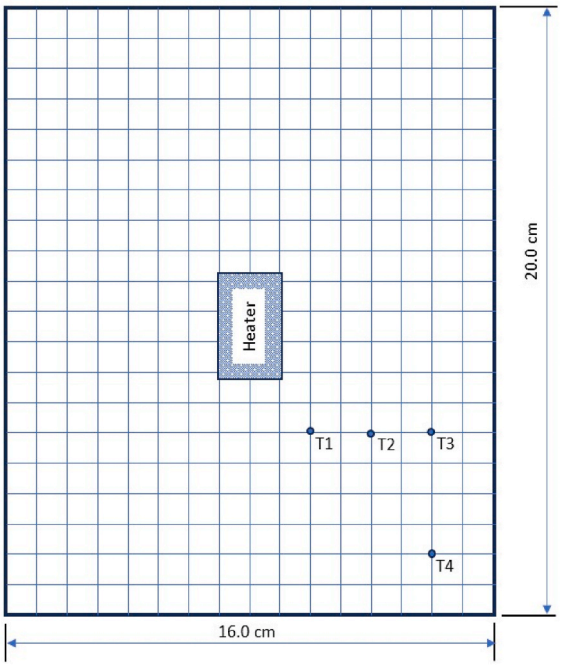


Fig. 8. Four temperature measurement locations: T1, T2, T3 and T4.

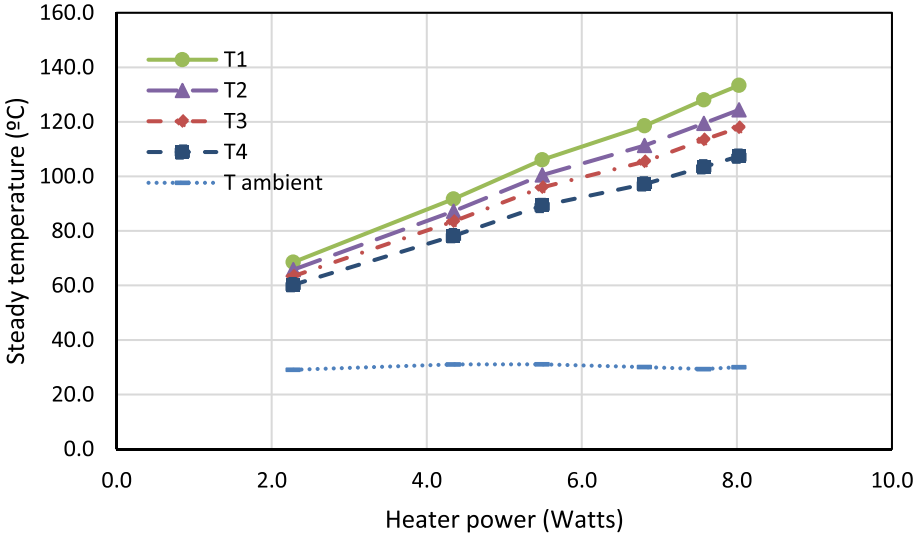


Fig. 9. Steady state temperatures for different heating powers.

3.2.2. Prediction of thermal conductivity of titanium plate

The effectiveness of the IHCP approach method was applied to the experimental data from the titanium plate specimen above. Table 3 shows the computational results for determining h_{diss} and k_p at each steady-state point. Fig. 10 illustrates the variation of h_{diss} with heater power. As the heater power increases, the plate temperature also increases, resulting in greater heat dissipation. Initially, the parameter h_{diss} changes significantly with increasing heater power. However, as the power increases further, the h_{diss} value tends to plateau. Environmental conditions may also contribute to the variation in h_{diss}. The temperature data acquisition system has been calibrated with an accuracy of ± 0.2 °C. Since there are four measurement points, the acceptable criterion is set at $\xi = 0.16$ (Equation (16)).

The thermal conductivity of titanium, as specified by the specimen vendor, is 17.0 W/m·°C. As shown in Table 3, the experimental k_p values are generally close to this reference. The data points yielded relatively satisfactory results, with deviations below 11.3 %. A trend is observed in which increasing the applied heater power results in predicted thermal conductivity values that more closely align

Table 3
Measurement results of k_p and h_{diss} for Titanium plate.

No	Daya (W)	h_{diss} (W/m^2.°C)	k_p -exp. (W/m.°C)	k_p -ref. (W/m.°C)	Absolute deviation of k_p (%)	S_{ML}	Decision
1	2.28	1.557	16.2	17.0	5.0	0.028	acceptable
2	4.35	1.938	18.6	17.0	9.3	0.025	acceptable
3	5.49	1.953	18.9	17.0	11.3	0.039	acceptable
4	6.81	2.099	18.2	17.0	7.1	0.063	acceptable
5	7.57	2.096	17.7	17.0	3.8	0.100	acceptable
6	8.03	2.124	17.6	17.0	3.8	0.086	acceptable

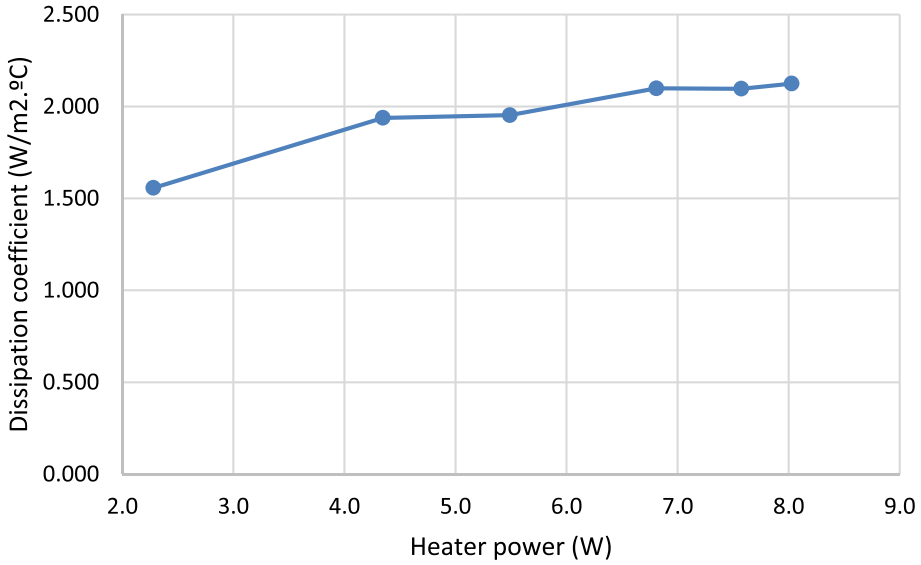


Fig. 10. Dissipation coefficient, h_{diss}, at various heating power levels.

with the vendor's reference (Fig. 11).

The dissipation coefficient plays a significant role in the calculation of heat transfer equations and becomes a major challenge in characterizing the thermal properties of materials. Literature studies show that in various methods for measuring thermal conductivity, identifying heat dissipation is a common source of inaccuracy. With the IHCP approach, both heat dissipation and material

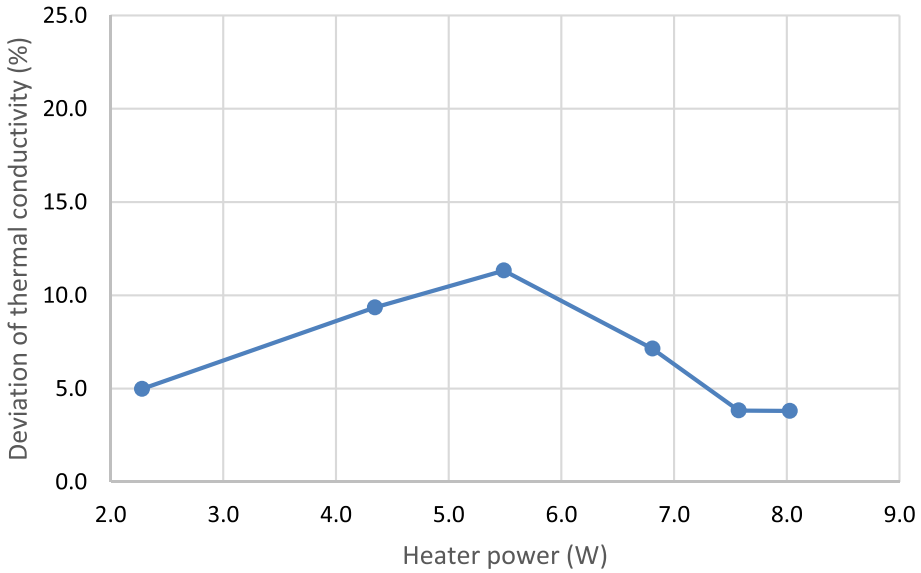


Fig. 11. Deviation in the measured thermal conductivity of the Titanium plate.

thermal conductivity are treated as unknown variables and can be solved simultaneously. In the developed algorithm, the variables h_{diss} and k_p are alternately solved as single variables, assuming the other is known. Through iterative computation, the thermal conductivity k_p of a material can ultimately be determined while simultaneously identifying the heat dissipation phenomena that occur. In conventional thermal conductivity measurements, a preliminary characterization step is typically required to identify heat losses to the environment. With the proposed method, such preliminary characterization is no longer necessary.

4. Conclusions

The method for measuring thermal conductivity has become an international standard procedure and continues to be developed to improve result precision. One of the challenges in such measurements is the identification of heat dissipation phenomena during testing. In this study, the IHCP approach has been developed to measure thermal conductivity while simultaneously identifying heat dissipation phenomena. This method was applied to synthetic data and demonstrated that the thermal properties of a material can be determined. Subsequently, the IHCP approach was applied to an experiment using a titanium plate. The numerical computation yielded relatively satisfactory results, with deviations below 11.3 %. There is a tendency that the higher the applied heater power, the closer the predicted thermal conductivity of titanium approaches the vendor's reference value. The measurement of a material's thermal conductivity using the IHCP approach can successfully identify both the material's thermal conductivity and its heat dissipation coefficient. As a result, prior characterization of heat dissipation is no longer required.

CRediT authorship contribution statement

Ari Satmoko: Writing – review & editing, Writing – original draft, Visualization, Software, Methodology, Investigation, Formal analysis, Conceptualization. **Engkos Achmad Kosasih:** Writing – review & editing, Supervision, Resources, Methodology, Funding acquisition, Conceptualization. **Anhar Riza Antariksawan:** Writing – review & editing, Supervision, Methodology, Formal analysis, Conceptualization. **Muhsin Kılıç:** Writing – review & editing, Formal analysis. **Ahmad Zikri:** Writing – review & editing, Visualization. **Muhammad Ainun Al Ghafari:** Writing – original draft, Investigation, Data curation. **Muflikh Kas Yudamaulana:** Project administration, Investigation, Data curation. **Seli Siti Sholihat:** Writing – review & editing, Validation, Formal analysis.

Declaration of competing interest

The authors declare the following financial interests/personal relationships which may be considered as potential competing interests: Achmad Engkos Kosasih reports financial support was provided by University of Indonesia. Achmad Engkos Kosasih reports a relationship with University of Indonesia that includes: board membership. If there are other authors, they declare that they have no known competing financial interests or personal relationships that could have appeared to influence the work reported in this paper.

Acknowledgement

This research was funded by Hibah Publikasi Terindeks International (PUTI) Q1 Tahun Anggaran 2024–2025, Nomor: NKB-482/UN2. RST/HKP.05.00/2024.

Data availability

Data will be made available on request.

References

[1] W. Zhao, Y. Yang, Z. Bao, D. Yan, Z. Zhu, Methods for Measuring the Effective Thermal Conductivity of Metal Hydride Beds: a Review, Elsevier Ltd., Feb. 28, 2020, https://doi.org/10.1016/j.ijhydene.2019.12.185.
[2] D. Kim, S. Lee, I. Yang, Verification of thermal conductivity measurements using guarded hot plate and heat flow meter methods, J. Kor. Phys. Soc. 78 (12) (Jun. 2021) 1196–1202, https://doi.org/10.1007/s40042-021-00177-0.
[3] K. Sun, C. Zheng, Y. Wu, W. Zhang, Experimental investigation on thermal conductivity of straw boards based on the temperature control box—heat flux meter method, Sustainability 15 (14) (Jul. 2023), https://doi.org/10.3390/su151410960.
[4] B. Feng, Y.H. Zhang, J. Tu, L.W. Fan, Z.T. Yu, Determination on the thermal conductivity and thermal contact resistance of thin composite phase change films as a thermal interfacial material, Case Stud. Therm. Eng. 33 (May 2022), https://doi.org/10.1016/j.csite.2022.101979.
[5] K.F. Wu, T.F. Cao, W. Bin Li, H. Zhang, G.H. Tang, Quantitative evaluation of the natural convection effect on thermal conductivity measurement with transient plane source method, Case Stud. Therm. Eng. 45 (May 2023), https://doi.org/10.1016/j.csite.2023.102933.
[6] I. Sánchez-Calderón, B. Merillas, V. Bernardo, M.Á. Rodríguez-Pérez, Methodology for measuring the thermal conductivity of insulating samples with small dimensions by heat flow meter technique, J. Therm. Anal. Calorim. 147 (22) (Nov. 2022) 12523–12533, https://doi.org/10.1007/s10973-022-11457-7.
[7] D. Zhao, X. Qian, X. Gu, S.A. Jajja, R. Yang, Measurement techniques for thermal conductivity and interfacial thermal conductance of bulk and thin film materials, J. Electron. Packag. 138 (4) (Dec. 2016), https://doi.org/10.1115/1.4034605.
[8] U. Hammerschmidt, J. Hameury, R. Strnad, E. Turzó-Andras, J. Wu, Critical review of industrial techniques for thermal-conductivity measurements of thermal insulation materials, Int. J. Thermophys. 36 (7) (Jul. 2015) 1530–1544, https://doi.org/10.1007/s10765-015-1863-x.
[9] M. Janek, J. Kudelcik, S. Hardon, M. Gutten, Novel, cost effective, and reliable method for thermal conductivity measurement, Sensors 24 (22) (Nov. 2024), https://doi.org/10.3390/s24227269.
[10] A. Satmoko, E.A. Kosasih, M.I. Dzaky, H. Abral, A.R. Antariksawan, A. Arafat, Application of the conjugate gradient method for predicting unknown heat flux in 2D plat under effect of insulation, J. Adv. Res. Fluid Mech. Therm. Sci. 110 (2) (2023) 176–191, https://doi.org/10.37934/arfmts.110.2.176191.

[11] R.N. Prithiviraajan, S. Somasundharam, K.S. Reddy, Development of experimental methodology for estimation of thermo-physical properties of engineering materials using inverse method, Therm. Sci. Eng. Prog. 22 (May 2021), https://doi.org/10.1016/j.tsep.2020.100832.
[12] J. Zhang, T. Lu, J. Deng, S. Ding, P. Xiong, Rapid identification of erosion thinning and scaling thickening of inner wall of circular tube based on inverse heat conduction problem method, Therm. Sci. Eng. Prog. 47 (Jan) (2024), https://doi.org/10.1016/j.tsep.2023.102263.
[13] M. Thomas, N. Boyard, N. Lefèvre, Y. Jarny, D. Delaunay, An experimental device for the simultaneous estimation of the thermal conductivity 3-D tensor and the specific heat of orthotropic composite materials, Int. J. Heat Mass Tran. 53 (23–24) (Nov. 2010) 5487–5498, https://doi.org/10.1016/j.ijheatmasstransfer.2010.07.008.
[14] S. Chanda, C. Balaji, S.P. Venkateshan, A. Ambirajan, V. Ramakrishnan, Simultaneous estimation of principal thermal conductivities of an anisotropic composite medium: an inverse analysis, J. Heat Tran. 135 (2) (2013), https://doi.org/10.1115/1.4007422.
[15] V. Maneesh, P.M. Kamath, A methodology to estimate thermal conductivity using inverse method, in: International Conference on Energy and Environment-2013 (ICEE 2013), Dec. 2013 [Online]. Available: www.ijirset.com.
[16] A. Saad, A. Echchelh, M. Hattabi, M. El Ganaoui, The identification of effective thermal conductivity for fibrous reinforcement composite by inverse method, J. Reinforc. Plast. Compos. 33 (23) (Dec. 2014) 2183–2191, https://doi.org/10.1177/0731684414556011.
[17] J. Zhang, G. Su, T. Chen, Estimating temperature-dependent thermal conductivity of copper oxide using an inverse method, J. Therm. Anal. Calorim. (Nov. 2024), https://doi.org/10.1007/s10973-024-13445-5.
[18] Y.M. Matsevytyi, V.V. Hanchyn, The solution of the inverse problem of identifying the thermal conductivity tensor in anisotropic materials, J. Mech. Eng. 24 (3) (Sep. 2021) 6–13, https://doi.org/10.15407/pmach2021.03.006.
[19] L. Yang, B. Sun, X. Sun, Inversion of thermal conductivity in two-dimensional unsteady-state heat transfer system based on finite difference method and artificial bee colony, Appl. Sci. (Switzerland) 9 (22) (Nov. 2019), https://doi.org/10.3390/app9224824.
[20] S. Somasundharam, K.S. Reddy, Simultaneous estimation of thermal properties of orthotropic material with non-intrusive measurement, Int. J. Heat Mass Tran. 126 (Nov. 2018) 1162–1177, https://doi.org/10.1016/j.ijheatmasstransfer.2018.05.061.
[21] S. Sun, Y. Ji, Z. Chang, G. Wang, L. Wei, Application of stochastic particle swarm optimization algorithm for noninvasive determination of temperature-dependent thermal properties of biological tissue, Heat Tran. Res. 53 (11) (2022) 45–60, https://doi.org/10.1615/HEATTRANSRES.V53.I11.40.
[22] S. Sun, Simultaneous reconstruction of thermal boundary condition and physical properties of participating medium, Int. J. Therm. Sci. 163 (May 2021), https://doi.org/10.1016/j.ijthermalsci.2021.106853.
[23] A. Satmoko, et al., Heat flux meter using 2D inverse heat conduction problem approach, Therm. Sci. Eng. Prog. 62 (Jun. 2025) 103622, https://doi.org/10.1016/j.tsep.2025.103622.
[24] Yunus A. Çengel, Afshin J. Ghajar, Heat and Mass Transfer Fundamentals and Applications, fifth ed., McGraw-Hill Education, 2015.
[25] M.N. Özisik, H.R.B. Orlande, Inverse Heat Transfer, second ed., CRC Press, 2021.